Senior Thesis

Baker Wood Creasoting Site Investigation using Geophysics

by
James Cox
1999

Submitted as partial fulfillment of
the requirements for the degree of
Bachelor of Sciencein Geological
Sciences at The Ohio State University,
Spring Quarter, 1999

Approved by:

Dr. Jeffrey Daniels

TABLE OF CONTENTS

page

LIST OF FIGURES

Abstract

Two geophysical techniques, Ground Penetrating Radar (GPR) and Electromagnetic (EM), were employed and compared at an industrial site that formerly operated as a creasote wood treating facility. The geophysical techniques were used for mapping the spatial extent of creasote contamination and to locate buried tanks, pipes and other subsurface features that could potentially lead to further contamination of the site if ruptured. While the EM data failed to image subsurface anomalies in the surveyed area, the GPR data proved successful in locating creasote-filled trenches, pipes, and buried tanks.

Introduction

Explanation of the Problem

The application of geophysics to detect presence and movement of hydrocarbons in the subsurface can be classified under two main headings: 1) readings made at fixed locations, as a function of time, are termed *monitoring,* and 2) *mapping* is the task of determining the spatial extent of contamination that already exist at a particular time. To monitor or map a site the host material conductivity must be known and contrasting from the hydrocarbons. Also the response to contamination must rise above reading errors and a natural scatter due to temporal changes in the conductivity structure such as water table variations.

Under favorable site conditions ground penetrating radar (GPR) and Electromagnetics (EM) have proven to be an effective tools for mapping and monitoring the spatial extent of contaminants. The contaminants must have a significant conductivity contrast with the native groundwater for EM to be able map and detect contaminates in the subsurface. For GPR, there needs to be a relative electric permittivity contrast between the host material and contaminants.

In 1988 the Ohio Environmental Protection Agency (Ohio EPA, 1999) became concerned about the Baker Wood Creosoting site, when some of the highest concentrations of polynuclear aromatic hydrocarbon compounds (PAH's) in the state were detected in the sediments of a surface water body near the site. Creosote contains PAH's which are large, flat compounds that are similar to benzene in structure and are carcinogenic compounds. Creosote was a common preservative used in the wood treating process

of railroad ties and telephone poles. GPR and EM systems, were employed to aid in the mapping of PAH's at the site.

Site Description and Site Conditions

As shown in figure 1, the Baker Wood Creasoting site consists of approximately 100 acres and is located on the western edge of the City of Marion, Marion County. The site is located in the northwest corner of the intersection of State Route 309 and Holland Road. Industrial to the south, residential and commercial to the east and north and agricultural to the west surrounds the site. The geographic coordinates for the site are 40 degrees, 35 minutes, and 37 seconds' north latitude and 83 degrees, 9 minutes, and 20 seconds west longitude.

Marion County lies in a glaciated region. During the Late Wisconsin, several advances and withdraws of the continental ice sheet left a layer of glacial debris over the county. 2 to 42 feet of glacial outwash sand and gravel directly overlie the bedrock. Over the sand and gravel is 14 to 59 feet of glacial till consisting of clay and silt with occasional fine sand lenses. The sand lenses within the till can potentially transport contaminants and ground water laterally (Morrison, 1918). The bedrock is composed of Columbus and Delaware, limestone, dolostone, and shale. They are at depths of 30 to 64 feet. The bedrock appears to contain a shallow and deep aquifer with depths ranging from 40 feet to 250 feet accordingly. The shallow aquifer is used for private residential wells while the deep aquifer is pumped for the municipal water supply (Ohio EPA Report, 1999).

Within the survey area there is still some remnants of the creasote operation, as Figure 2 shows. There are four creasote tank pads seen on the surface and consist of cement. There is asphalt present in the S-SW area of the site. Also there is remnants of the old pump house.

Ground Penetrating Radar Measurements

Ground Penetrating Radar (GPR) is a geophysical technique commonly used to image the shallow subsurface of the earth. The principles and theory of GPR are based on the wave equation derived from

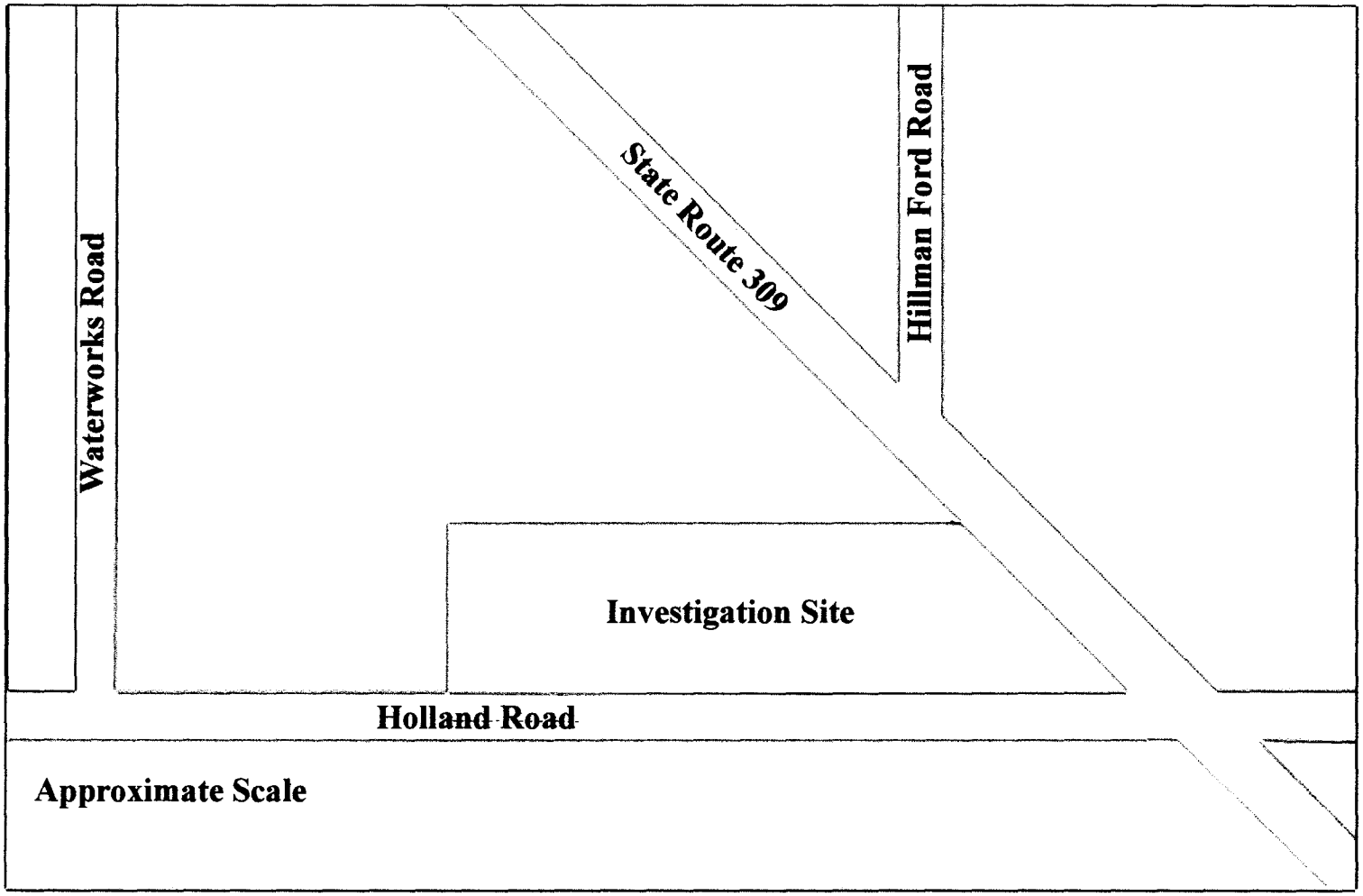

Figure 1
The location of the site surveyed in Marion, Oh.

(a)

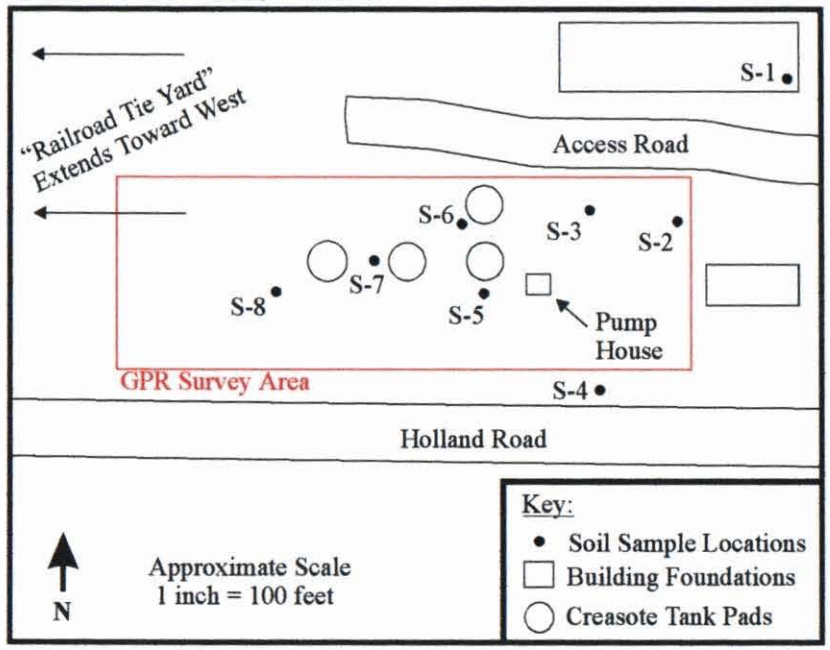

(b)

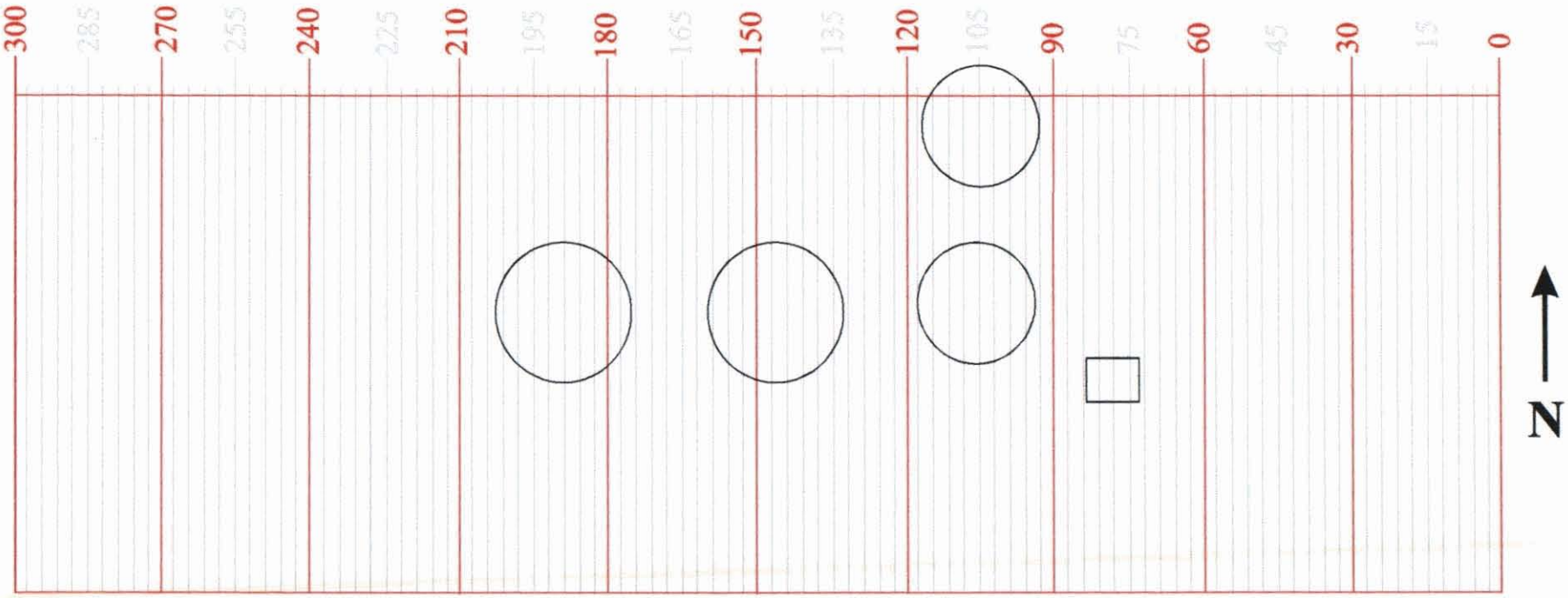

Figure 2

(a) Baker Wood Creasote site and the surveyed area in Marion, Oh. (b) Details of the surveyed area.

Maxwell's Equation for electromagnetic wave propagation and the antenna design from field-testing (Daniels, 1989).

The principle of GPR is conceptually summarized in Figure 3. A typical GPR survey may involve two antennas, where one antenna transmits and the other receives, this is called a bistatic system. The transmit antenna radiates a short pulse of electromagnetic energy in the 25MHz to 1GHz frequency range into the ground. The energy propagates down through the subsurface and is reflected, refracted, or diffracted at boundaries of electrical and magnetic property contrasts within the earth and is called an impedance contrast. When the transmit antenna is activated, "a trigger impulse opens a channel to record the voltages arriving on the input cable attached to the receiver antenna," (Roberts, 1994). The receive antenna is sensitive to waves that are directed towards the surface and along the long axis of the antenna. Commonly, the voltage oscillations recorded from the receive antenna are called reflections when interpreting the data even though the received signal may be composed of energy that are reflected, refracted, or diffracted at appropriate boundaries. In some instances a single antenna is used to transmit and receive the reflected energy and this mode of operation is called monostatic.

Scattering from subsurface features is recorded over a chosen time interval and depends on the propagation velocity of the wave through the material it is traveling in. The propagation velocity of electromagnetic waves is approximately inversely proportional to the square root of the relative permittivity of the ground:

$$Vp = C/(\epsilon r)^{0.5} \qquad (1)$$

where, Vp is the propagation velocity in meters/second, C is the velocity of a wave in air (the speed of light), and ϵr is the relative permittivity of the ground. So a low relative permittivity yields a high velocity and a high relative permittivity yields a lower velocity. Figure 4 gives some observed field relative permittivity values. Notice that the observed propagation velocity decreases when the medium is saturated with water.

The reflected pulse that is recorded by the receiver antenna is delayed by an amount of time that is a function of the propagation velocity and the depth of the electrical impedance contrast, according to the equation:

$$Td = 2(Z/Vp) \qquad (2)$$

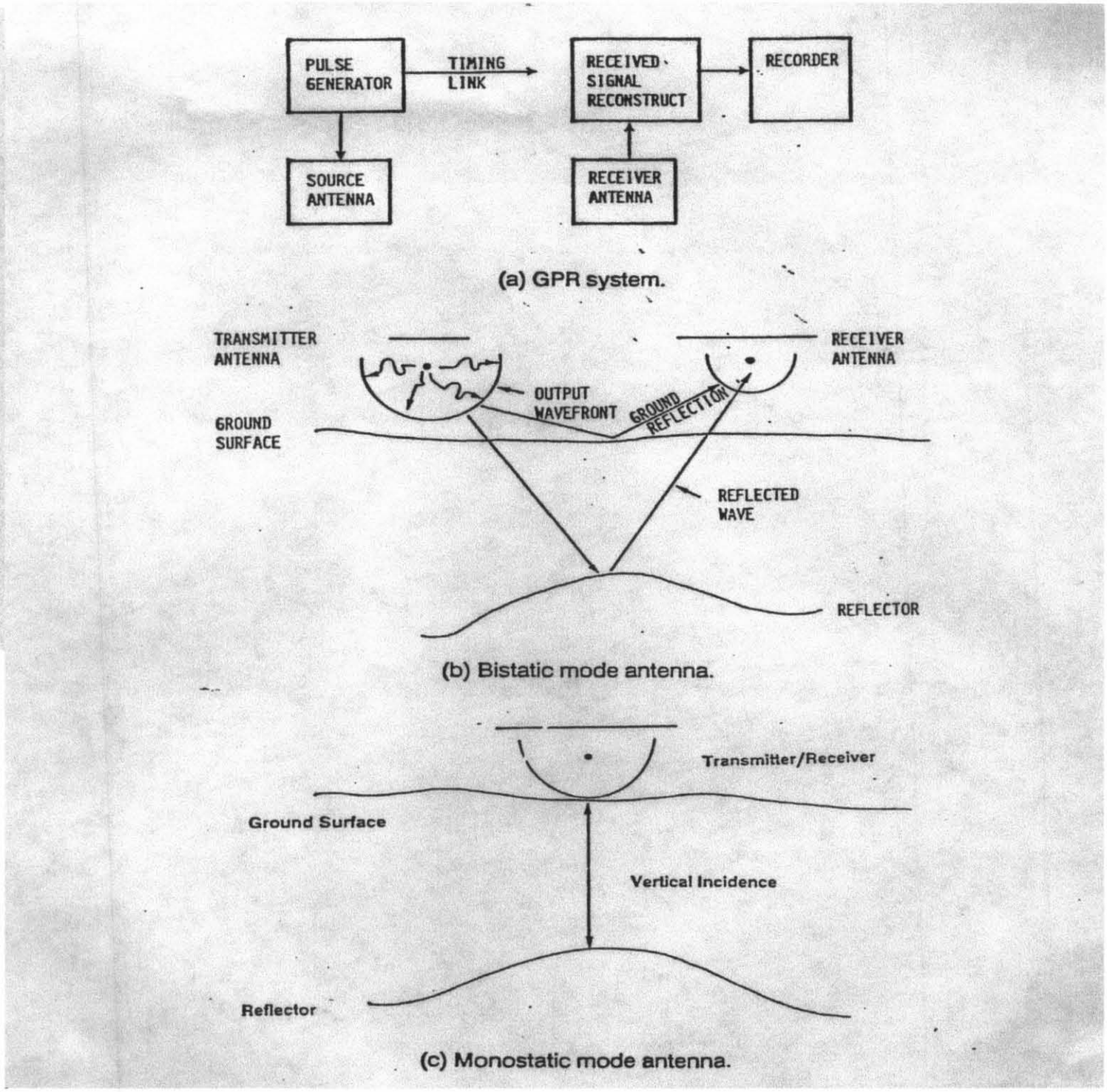

Figure 3

Operating components and modes of GPR. (a) Generalized diagram of GPR components. (b) Biastatic antenna operating mode. (c) Monostatic antenna operating mode (Daniels, 1989).

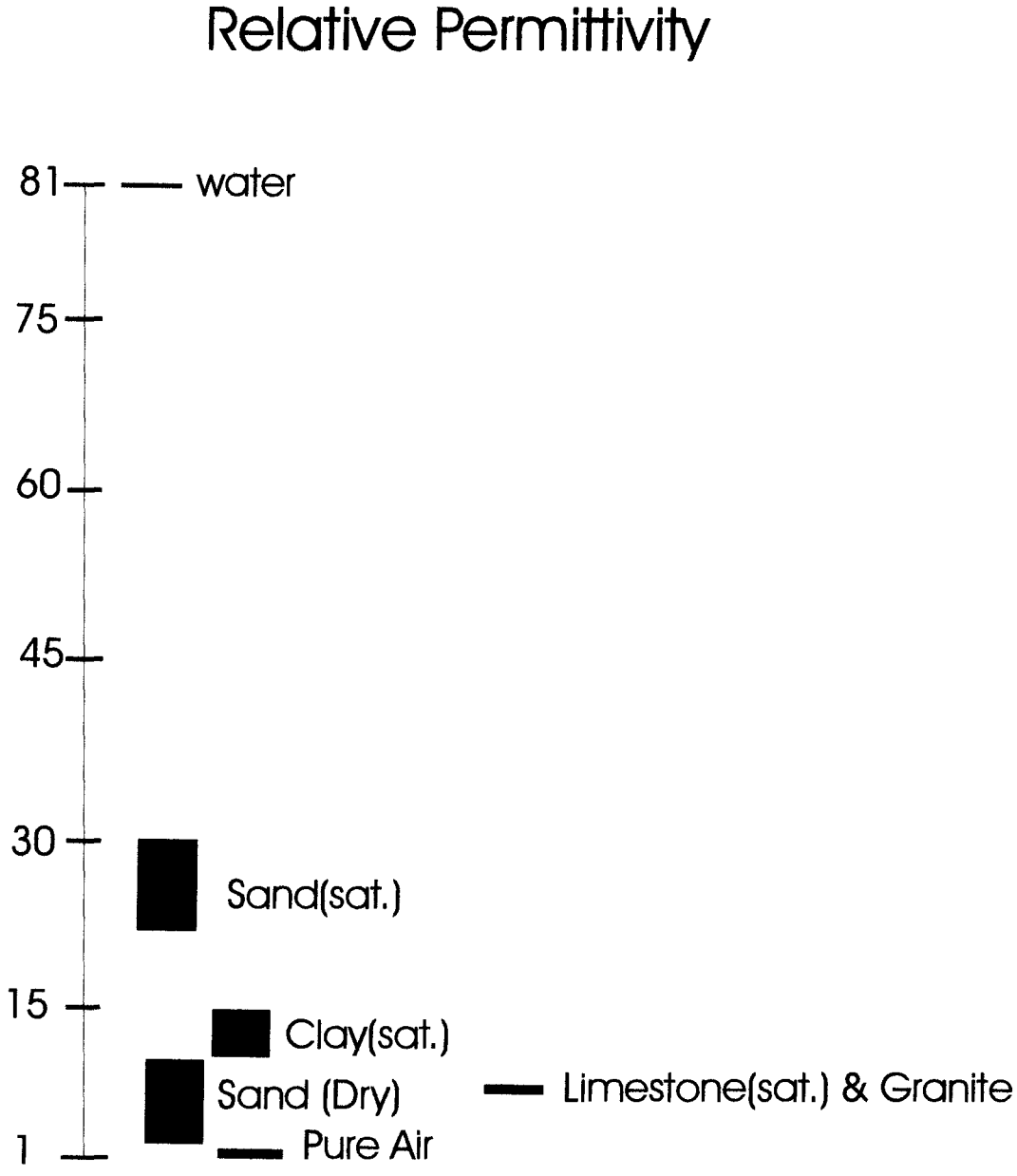

Figure 4
Some observed field permittivity with a porosity of 30%.

where Td is the two way travel time in nanoseconds, Z is the depth to target in meters, and Vp is the propagation velocity. The two way time represents the total time required for the incident and the refracted pulse to travel through the host rock. The typical length of the total recording time is between 10 and 1000 ns (Daniels, 1989).

Noise or clutter masks reflections from impedance contrasts and can make GPR data hard to interpret. Sources of clutter include reflection from aboveground objects, radio-frequency interference from nearby radio or television stations, any unwanted reflections, and antenna ringing. Filtering and stacking the data can often remove the unwanted clutter.

Most GPR systems employ dipole or bow-tie shaped antennas which radiate linearly polarized waves, as shown in Figure 5. Polarization is the alignment of the antenna and the electromagnetic waves, with the electric field vector parallel to the long axis of the antenna. An electromagnetic plane wave propagating through a homogeneous and isotropic medium contains electric and magnetic field vectors oriented transverse relative to the direction of propagation and perpendicular to each other. A unit vector is assigned to the electric field and its path determines the polarization of the electromagnetic wave. If the vector stays in the same plane as transmitted, then it is linearly polarized. If the electric and magnetic fields vector rotates around an axis parallel to the propagation direction, then the wave is elliptically polarized (Roberts, 1994).

The polarization of electromagnetic waves reflected or diffracted at an impedance contrast may or may not be the same polarization as the incident wave. The change in the polarization depends upon the angle of incidence, the impedance contrast, the antenna separation, and the shape and orientation of the target. If the polarization of the reflected or diffracted wave changes, then the electromagnetic wave is said to be depolarized. The receiver antenna is most sensitive to the electric field vector parallel to its long axis. If the polarization of the reflected wave is the same as the incident wave, then an antenna oriented parallel would detect the radiated energy, according to the reciprocity theorem. The reciprocity theorem applied to antennas states that the receiving pattern is identical to its transmitting pattern. If the reflected wave is depolarized, then an antenna oriented perpendicular would detect the radiated energy.

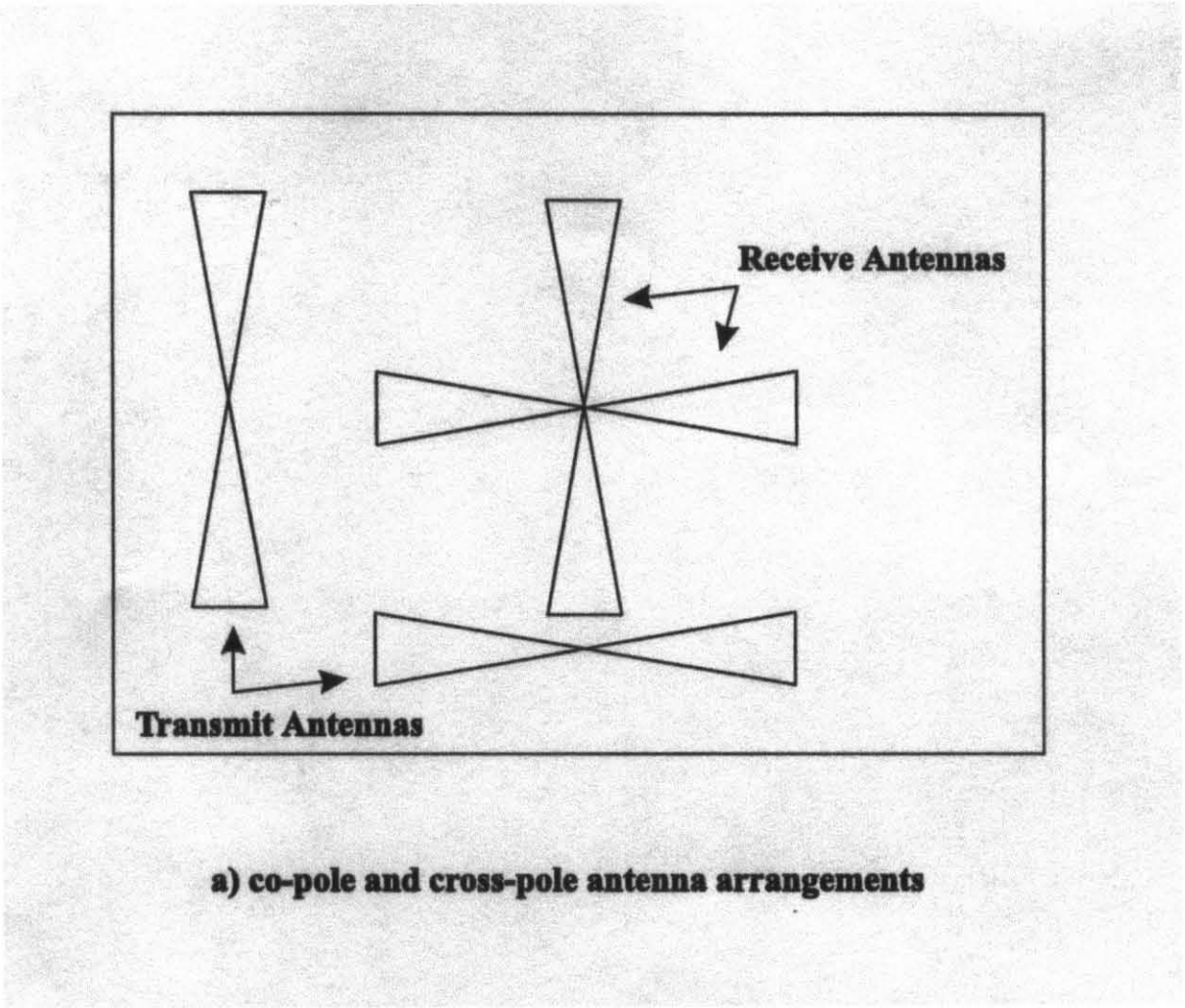

Figure 5
(a) Co-pole and cross-pole antenna arrangements.

Induced Electromagnetic Measurements

Electromagnetic (EM) measurements have the same theoretical basis in Maxwells equations that GPR measurements have, but EM operates in the lower frequency range (< 1MHz) where electrical conduction dominates electromagnetic propagation. EM equipment operates in the frequency domain at frequencies from 100 Hz to 10 MHz. At low frequency the eddy currents are deep within the earth. At high frequency the eddy currents are at the surface of the earth. EM equipment functions by generating a electromagnetic field called the primary field (Hp), induces a secondary magnetic (Hs) field in the earth called the secondary field, as conceptualized in figure 6. Generally the magnetic field (Hp and Hs) are converted to apparent conductivity values, rather than the associated electric field strength. Alternating current in a coil induces an alternating magnetic field, which extends through the surrounding region. If the region contains a conductive body, the primary field induces an alternating secondary currents to flow within the conductive body. The currents will usually flow through the conductor in planes perpendicular to the lines of magnetic field of force from the transmitter, unless restricted by the conductor's geometry (Klein and Lajoie, 1980). The ground current induces another alternating magnetic field, called the secondary field, which also extends through the region that includes the receiver. The total electromagnetic field around the receiver is the primary and the secondary fields. The combined magnetic field induces an alternating current in the receiver coil, which is measured and recorded.

Field Surveys and Data Processing

GPR Field Measurements

GPR was employed on Feb. 14, 1999 at the Baker Wood Creasoting site near Marion, Oh. to map the spatial extent of creasote contamination. The GPR system employed was a GSSI SIR-10 operating system and a bistatic 500 MHz center band antennas. A band pass filter was applied to reduce the amplitude of the reflected electromagnetic waves and the sample interval was 512 samples per trace. The antennas were attached to a

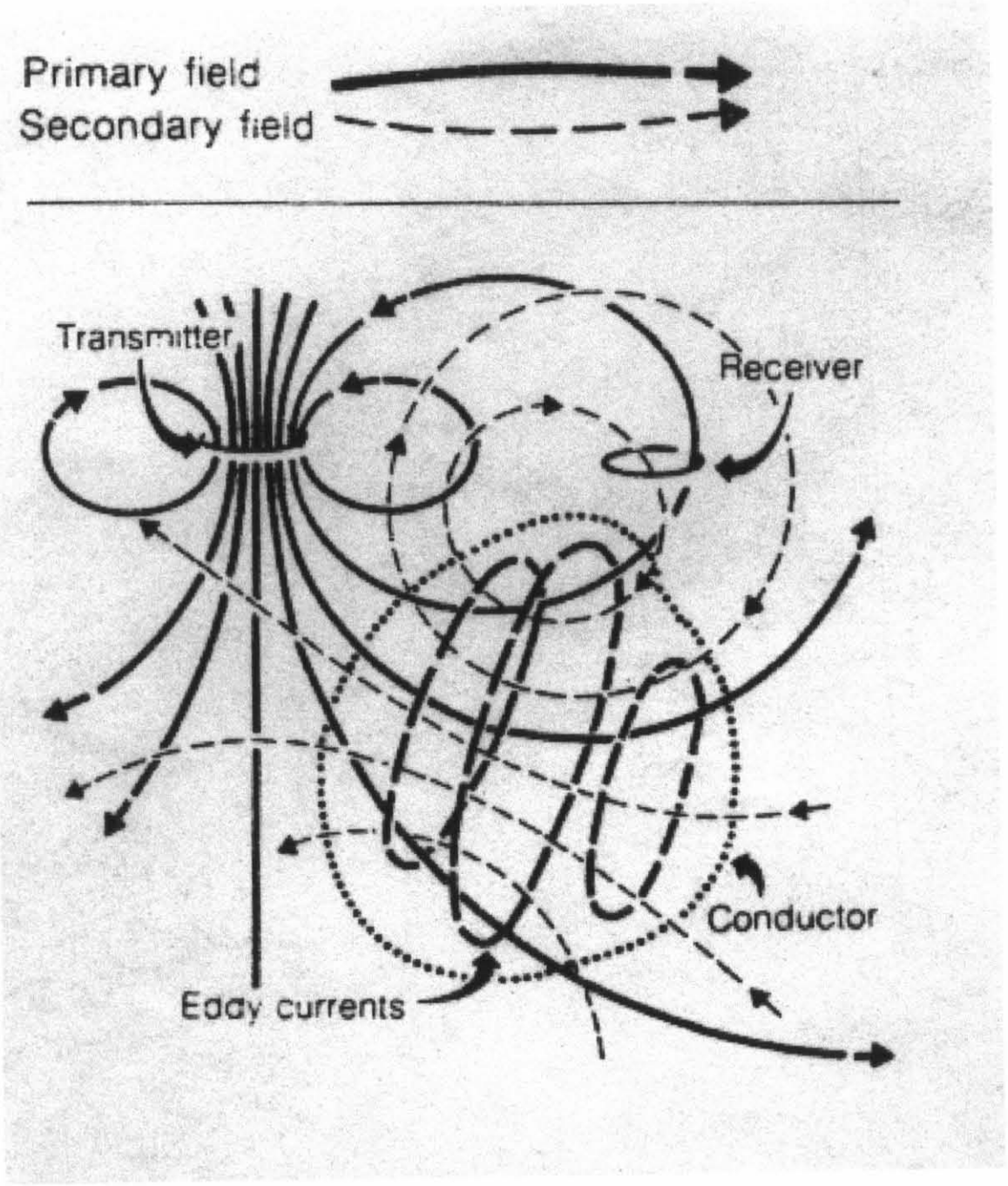

Figure 6

Generalized picture of electromagnetic induction (Klein, 1980).

sled and pulled by hand. Attached to the sled containing the antennas was a wheel which activated the antennas to record 4.55 traces per foot.

Figure 5 shows the arrangement and orientation of the antennas employed. The bow-tie antennas are arranged so that the mode of operation is monostatic and the system is co-polar and cross-polar. Both the co-pole and the cross-pole voltage oscillations were record at the same time but on different channels.

The GPR measurements were made on a 300 feet by 100 feet two-dimensional surface grid, with profile line running N-S, as shown in figure 2. The spacing between profile lines was three feet and was determined arbitrarily, not by the size of any subsurface objects.

EM Field Measurements

The GEM EM system was also employed at the Baker Wood Creasote site on the 4/14/99. The GEM system is a multi-frequency electromagnetic system that is manufactured by Geophex. The instrument is approximately 5.5 feet long and weighs approximately 10 pounds. The GEM system has a transmitting and receiving coils located at either end of the instrument. Also the instrument has a third coil that nulls the primary field and only the secondary magnetic field is seen. The secondary magnetic field induces an alternating current in the receiver coil, which is measured and recorded. Also, the operating frequency can be changed and up to five frequencies can be measured at one time.

The GEM system takes two readings of the magnetic field. The first is the quadrature component or the out-of-phase, which is related to the ground conductivity. It is a measurement of the amplitude of the field that is 90 degrees out of phase with the primary field. The second is the real component or in-phase, which is the measurement of the amplitude of the field that is in-phase with the primary field and is more sensitive to metal objects. The EM measurements were made along the same 300 feet by 100 feet two-dimensional surface grid as the GPR measurements were made. The measurements were made every two feet along a profile line, with frequencies of 2, 4, and 9 kHz.

GPR Data Processing and Display

The GPR measurements collected at the Baker Wood Creasoting site, were processed by a program called RADICAL (Grumman, 1995). Data processing included the following: 1) byte-swapping,

which is a step that must be preformed on data recorded on any IBM-based PC or on data produced on DEC computers before the data can be read by Silicon Graphics, Inc. (SGI) workstations. Byte-swapping converts the operating system used by DOS and DEC to the SGI format. 2) A one-dimensional filter with a bandwidth of 75 MHz to 600 MHz was applied to each trace. One-dimensional filtering simply smoothes the data and removes the DC component of the signal. 3) The gain was changed to make the data easier to view at later times in the section.

A "trace" of data is a recording of reflections arriving at the receiving antenna over a chosen time interval and at one transmit-receive antenna location. A profile line of data is obtained by recording successive traces at even distance increments as the antennas are moved over the ground. GPR traces along a profile line can easily be displayed side-by-side to form a gray-scale image, sometimes called a cross-section. Figure 8 conceptualizes a gray-scale image of profile line 180 from the Baker Wood Creasoting site. Assigning a shade of gray to amplitude ranges and placing successive traces of a line side by side creates gray-scale displays. Also GPR measurements made along two-dimensional profile lines can be displayed in three-dimensional perspective view and the construction of a three-dimensional image is conceptualized in Figure 7. Displaying successive profile lines side by side, sometimes referred to as a two-dimensional series, yields a three-dimensional image of the subsurface.

There are two basic requirements for accurate and meaningful display of three-dimensional data: 1) the GPR sample points should be accurately reproduced on the display, and 2) the data should be displayed in a semi-transparent manner (Daniels, 1997). The first requirement can be achieved by employing a voxel display, which honors each data point with equal weight. The second requirement can be achieved by employing a system that applies a volume-rendering algorithm to display the data in a semi-transparent perspective view. The algorithm employed in the following displays is called alpha rendering and the voxel display program is called BOB (Bob, 1995).

Data that is properly displayed in three-dimensions is readily interpretable, but the following factors must be taken into consideration to achieve this: 1) the optimum viewing angle of the display, 2) the amount of data that can be displayed, and 3) the amplitude-color assignments. The optimum viewing angle

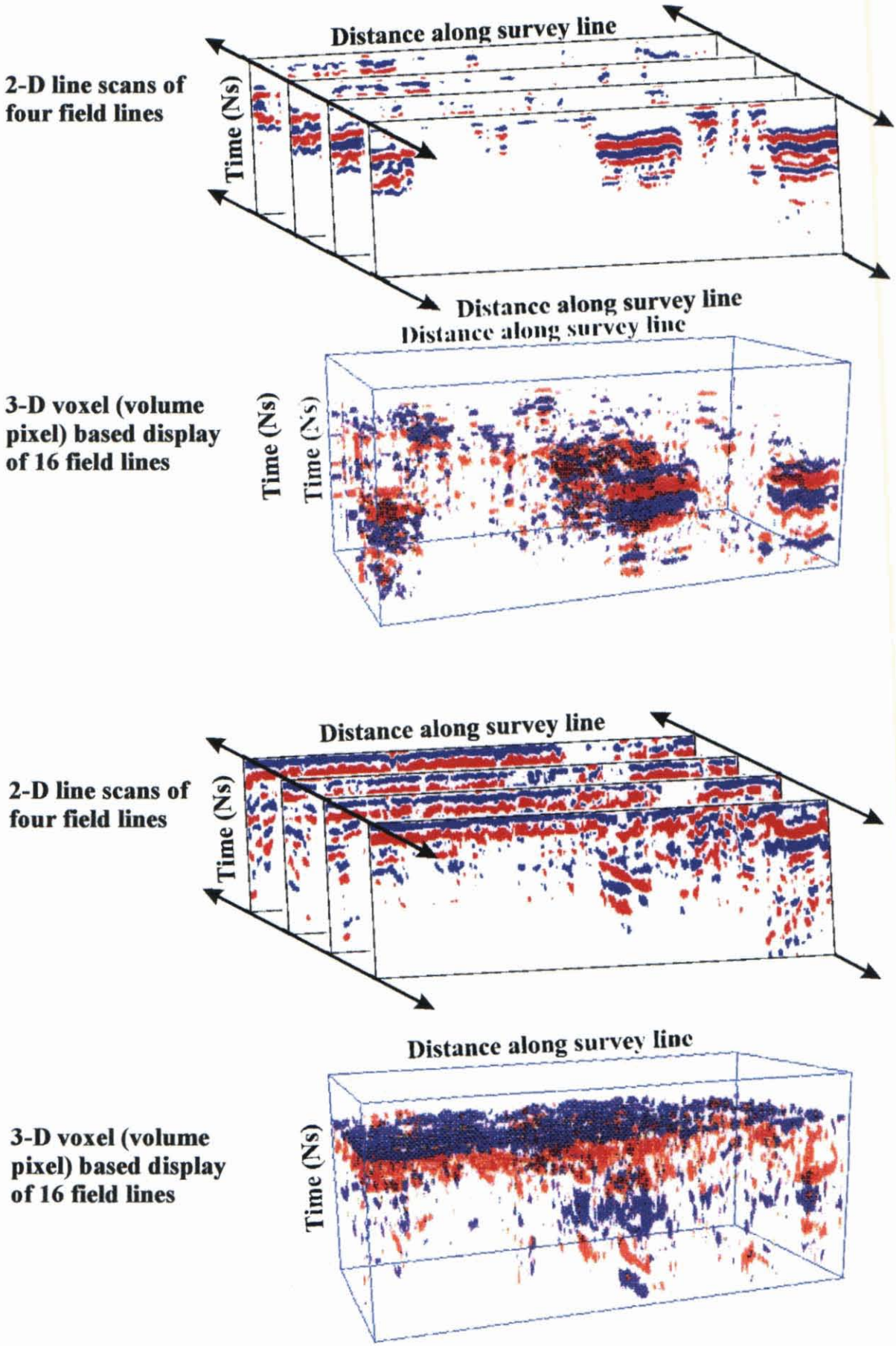

Figure 7

The construction of a three-dimensional GPR image.

is a matter of individual preference, but does vary with the complexity and orientation of the anomalies within the data. Often interpreters of geophysical data have a tendency to display more detail so not to miss any objects. The result is an image which the object of investigation is masked by noise or clutter. The image display parameters need to be kept as simple as possible in order to isolate and interpret the objects. A crucial part of the interpretation processes is the assignment of amplitude-color. An image display of a subsurface object can greatly be enhanced by not displaying the lower amplitudes or by displaying only one polarity.

EM Data Reduction and Display

There was not much processing needed to improve the EM measurements. In the data there is a DC shift, which happened when the instrument was turned off and then back on and had to be removed. According to Jeffrey J. Daniels, this DC shift was probably caused by change in temperature. The instrument started off cold and was used. Then after some time, the instrument was turned off and then on again at a different temperature.

EM can be displayed as in and out-of-phase profiles. The GEM system takes two readings of the secondary magnetic field. These two measurements can be plotted on a graph on the y-axis and the position or station on the x-axis, as in figures 8 and 9. Also EM measurements can be displayed as a contour map to create an image of the spatial extent of hydrocarbons. A contour map is a two-dimensional representation of three-dimensional data. Contours define lines of equal Z values across the extent of the map. The shape of the anomaly or anomalies is shown by the contour lines.

Surfer (Keckler, 1995) was the program employed to create the contour displays of the EM data in figures 10 and 11. Surfer is a rectangular grid-based contouring program and requires a grid file be generated from the EM data set. A grid is rectangular region comprised of evenly spaced rows and columns or X grid lines and Y grid lines respectively. The intersection of the lines defines the location of the grid nodes on a contour map. Because the EM data was collected on regular intervals and in a grid manner a grid file is produce that uses the Z values directly and does not interpolated the values for the grid nodes.

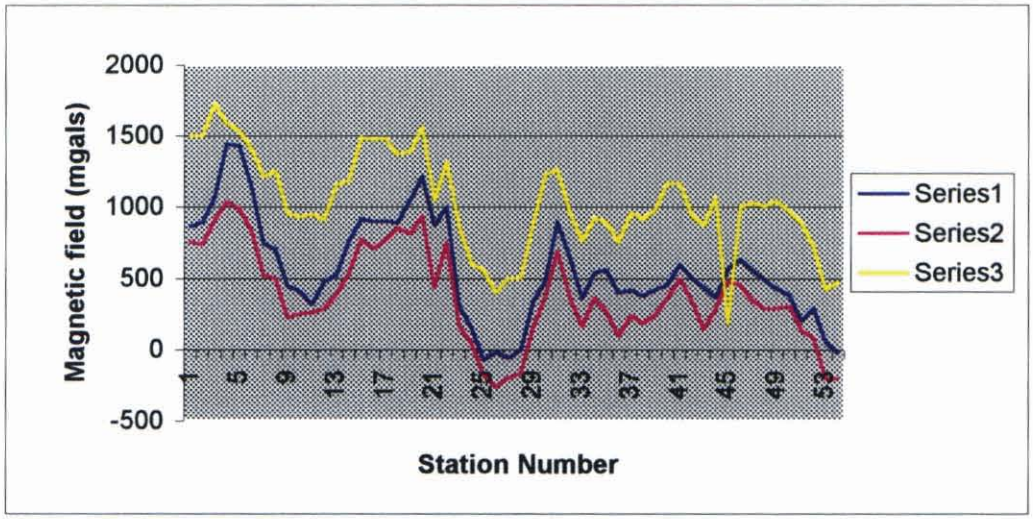

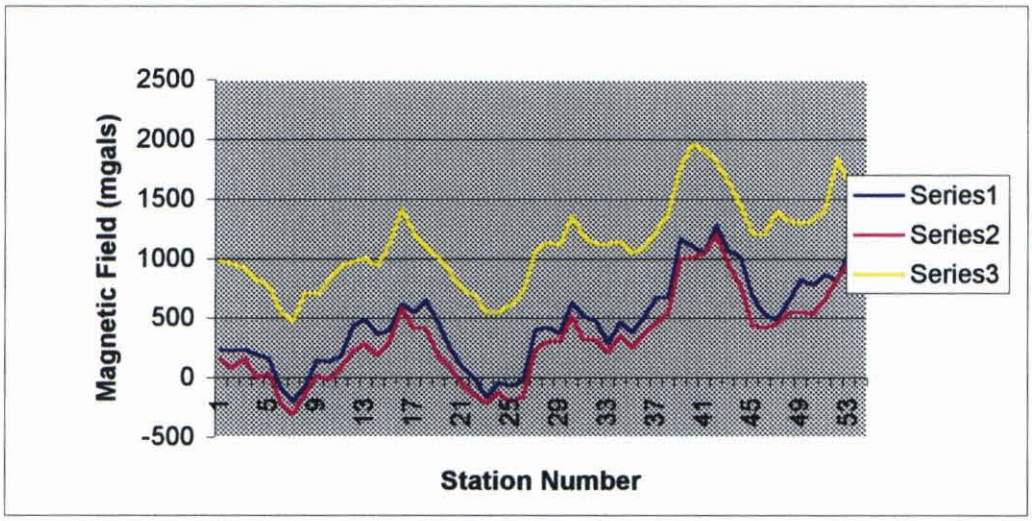

(b)

Figure 8

The measured secondary field (a) along profile line105, (b) along profiloe line 138, where series 1 is 2kHz, series 2 is 4kHz, and series 3 is 9kHz.

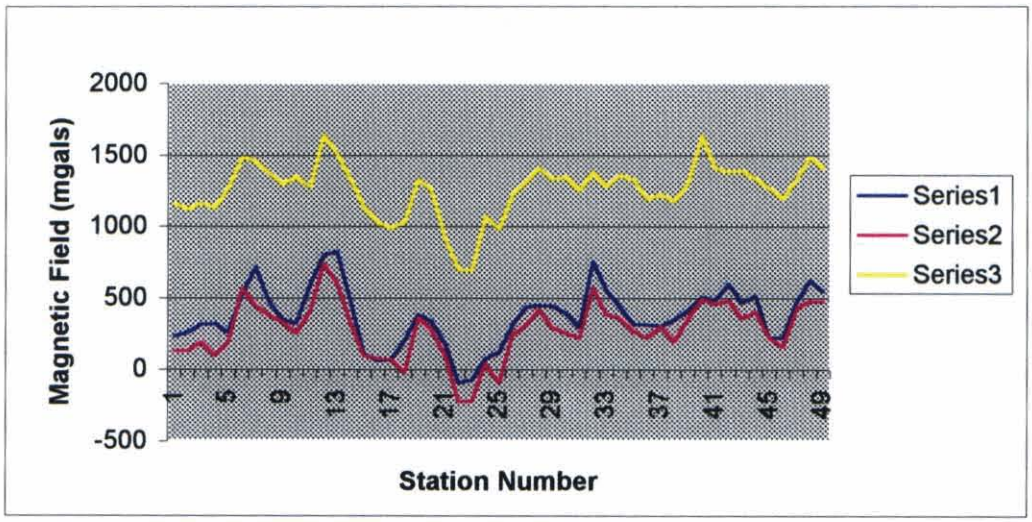

Figure 9
The measured secondary field along profile line 180, where series 1 is 2kHz, series 2 is 4kHz, and series 3 is 9kHz.

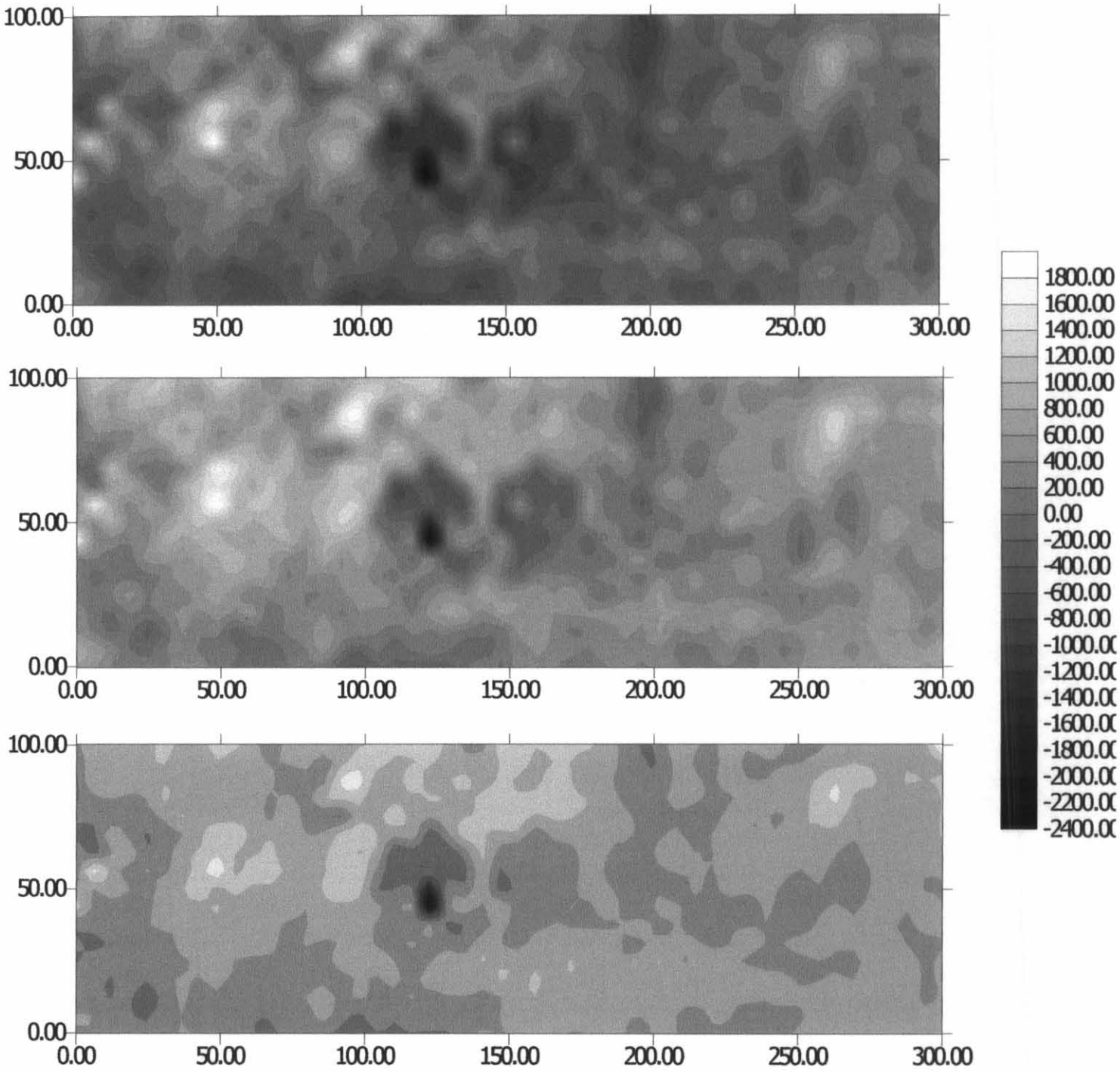

Figure 10

The in-phase contour maps of the EM data

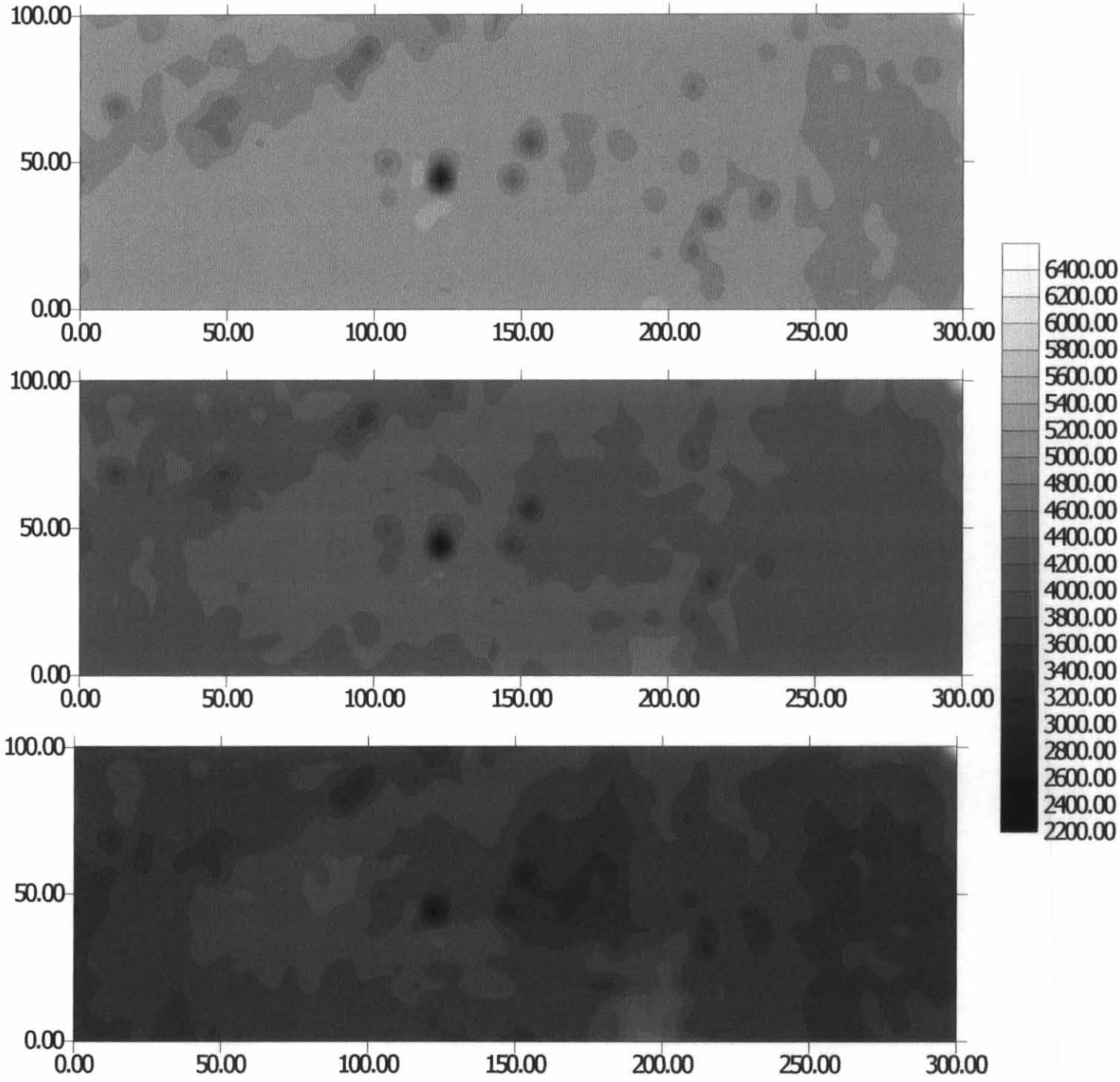

Figure 11

The out-of-phase contour maps of the EM data.

Ground Penetrating Radar Results

Two Dimensional and Three Dimensional Display and Interpretation

The presence of clutter and noise can make GPR data hard to interpret. The co-pole data recorded at the site contained a high amount of clutter as a result of soil layering and near-surface water. The cross-pole data recorded has much less clutter and a better signal to noise ratio. This is because the cross-pole is less sensitive to near surface layer and more sensitive to non-planer and rough objects (Guy, 1999).

Because of the clutter and noise present on the co-polar data, the cross-polar data was used for imaging the subsurface. Within then the cross-polar data there still is some noise present. There is near-surface water and high frequency radio wave noise from a near by radio antenna. The two-dimensional image in figure 12 has an anomaly between 75' and 90' on profile line 54. It is interpreted (later confirmed) as a creosote-filled pit.

Figure 13 is a two-dimensional image with several reflections and anomalies to interpret. There are two huge areas of reflections between 0' and 17', 35' and 45', and 90'and 100' of profile line 105. These three areas represent the creosote tank pads. Within two of the reflections of the creosote tank pads and at times of 15 ns (for the pad between 0' and 17') and 9 ns (for the pad between 35' and 45'), there small hyperbolas. These small hyperbolas are interpreted as rebars in the cement of the creosote tank pad. A pipe is detected in the two-dimensional GPR image and the shape of the anomaly indicated that is a pipe. Also underneath one of the creosote tank pad is a creosote filled pit.

Figure 14 shows an anomaly between 23' and 60' of profile line 138. Due to the shape of the anomaly and the presence of rebar, the anomaly is interpreted as a creosote tank pad.

Figure 15 shows a three-dimensional image of the subsurface at the Baker Wood Creosoting site and shows how readily they are interpretable. The tank pads are clearly seen in the image and are labeled 1-4 targets. The creosote-filling pit is readily seen in the three-dimensional image and labeled target 5.

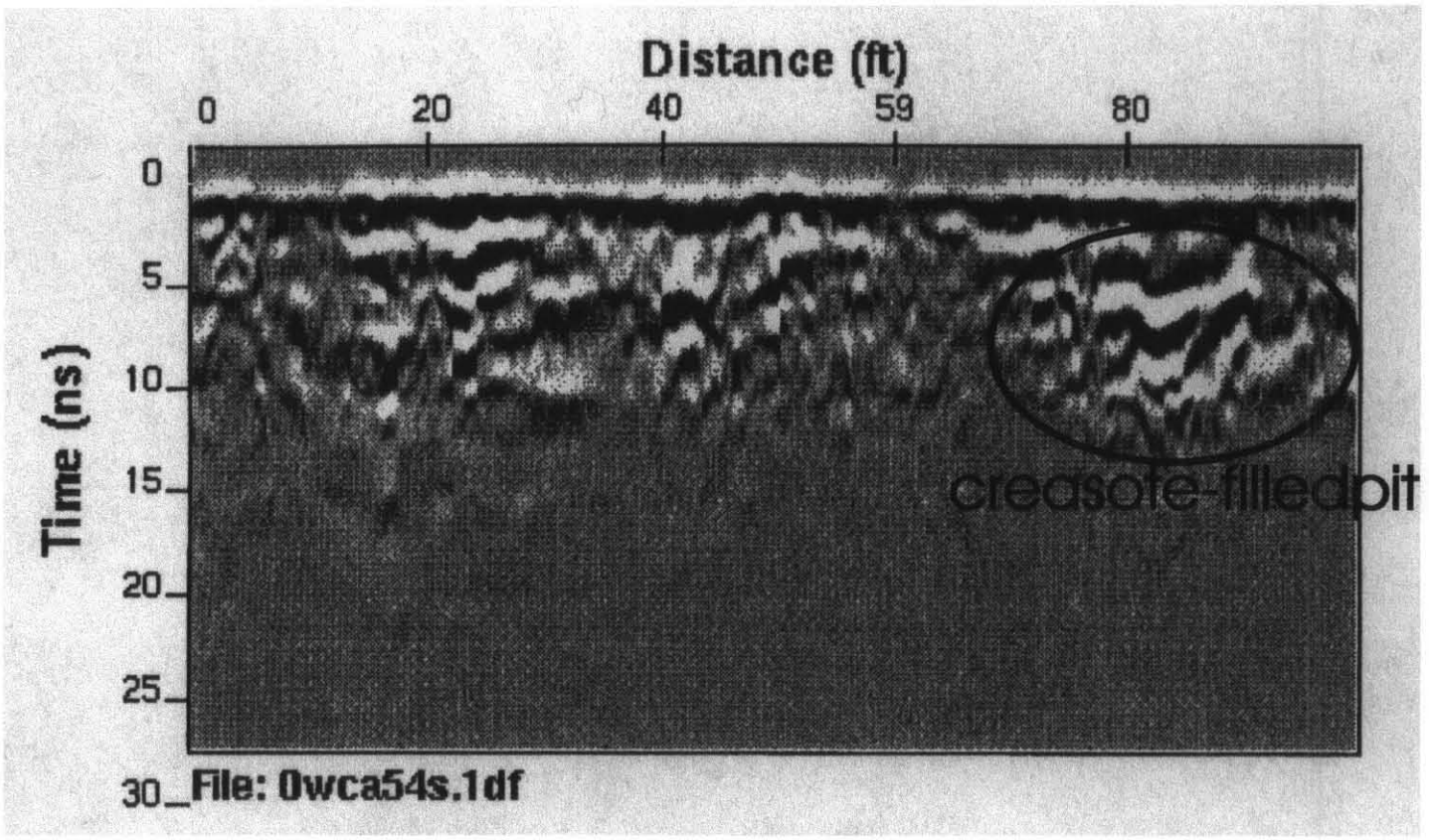

figure 12
A two-dimensional GPR image of profile line 54 showing a creasote-filled pit.

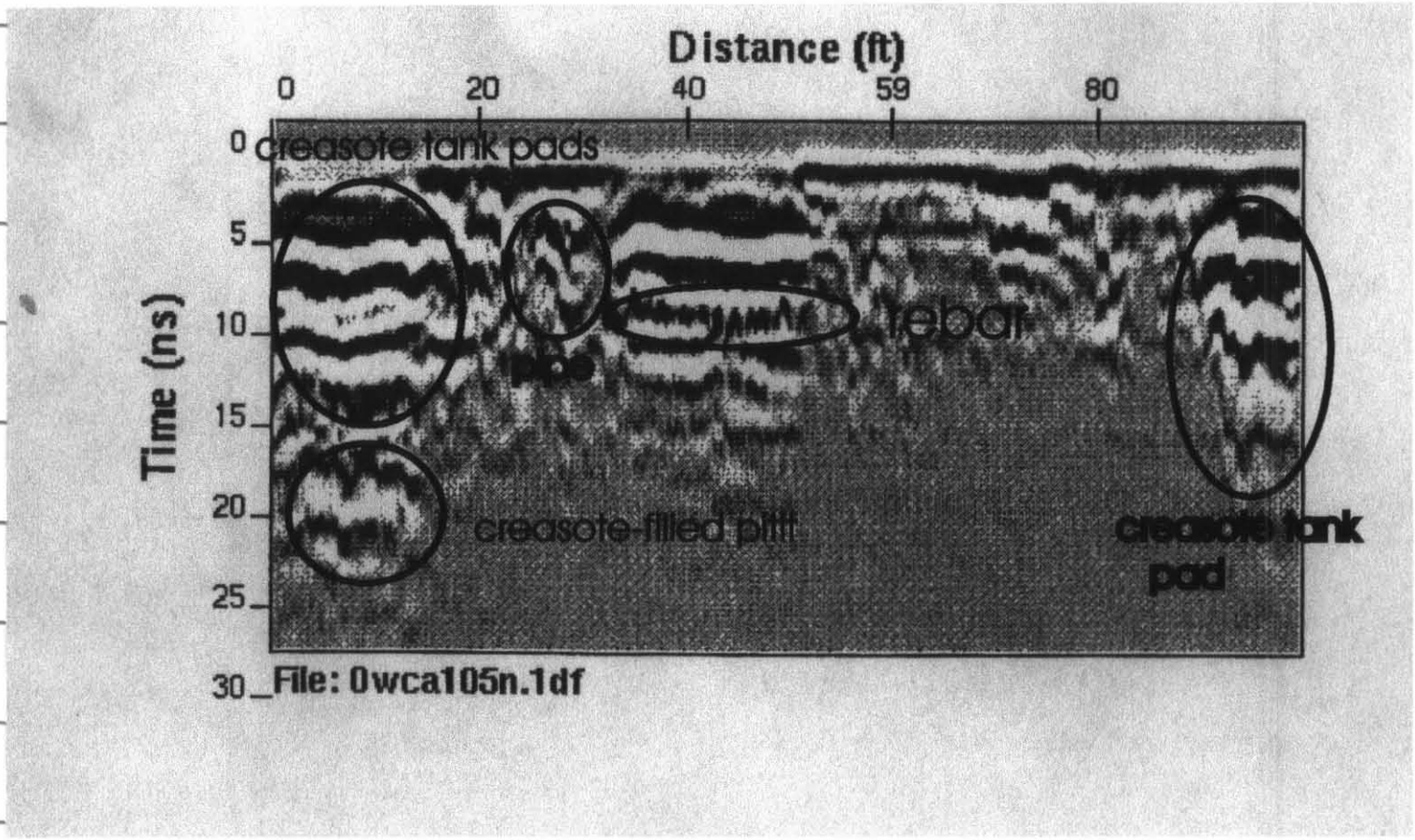

Figure 13
A two-dimensional GPR image of profile line 105 showing three creasote tank pads, a pipe, rebar, and a creasote-filled pit.

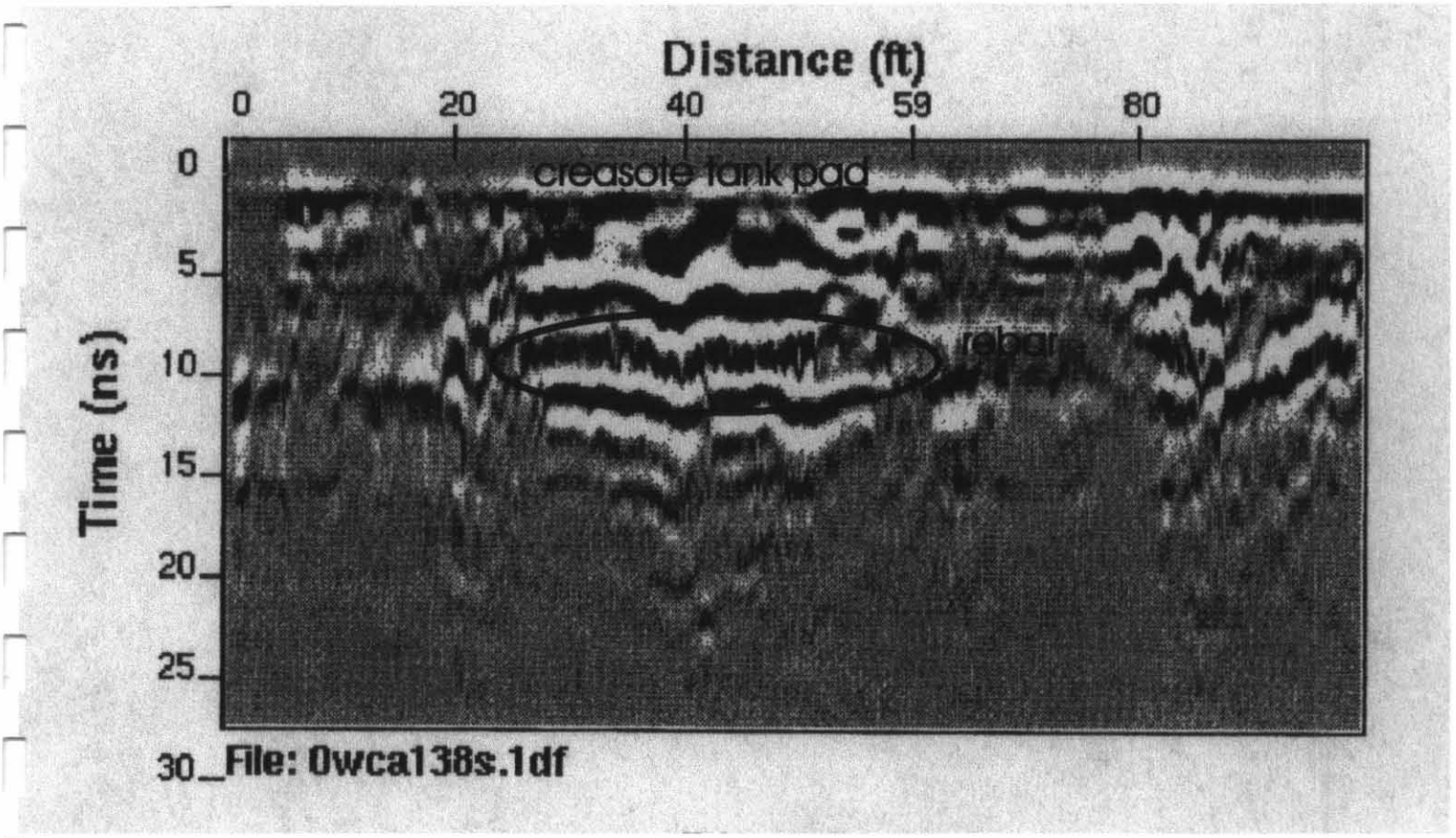

Figure 14
A two-dimensional GPR image of profile line 138 showing a creasote tank pad.

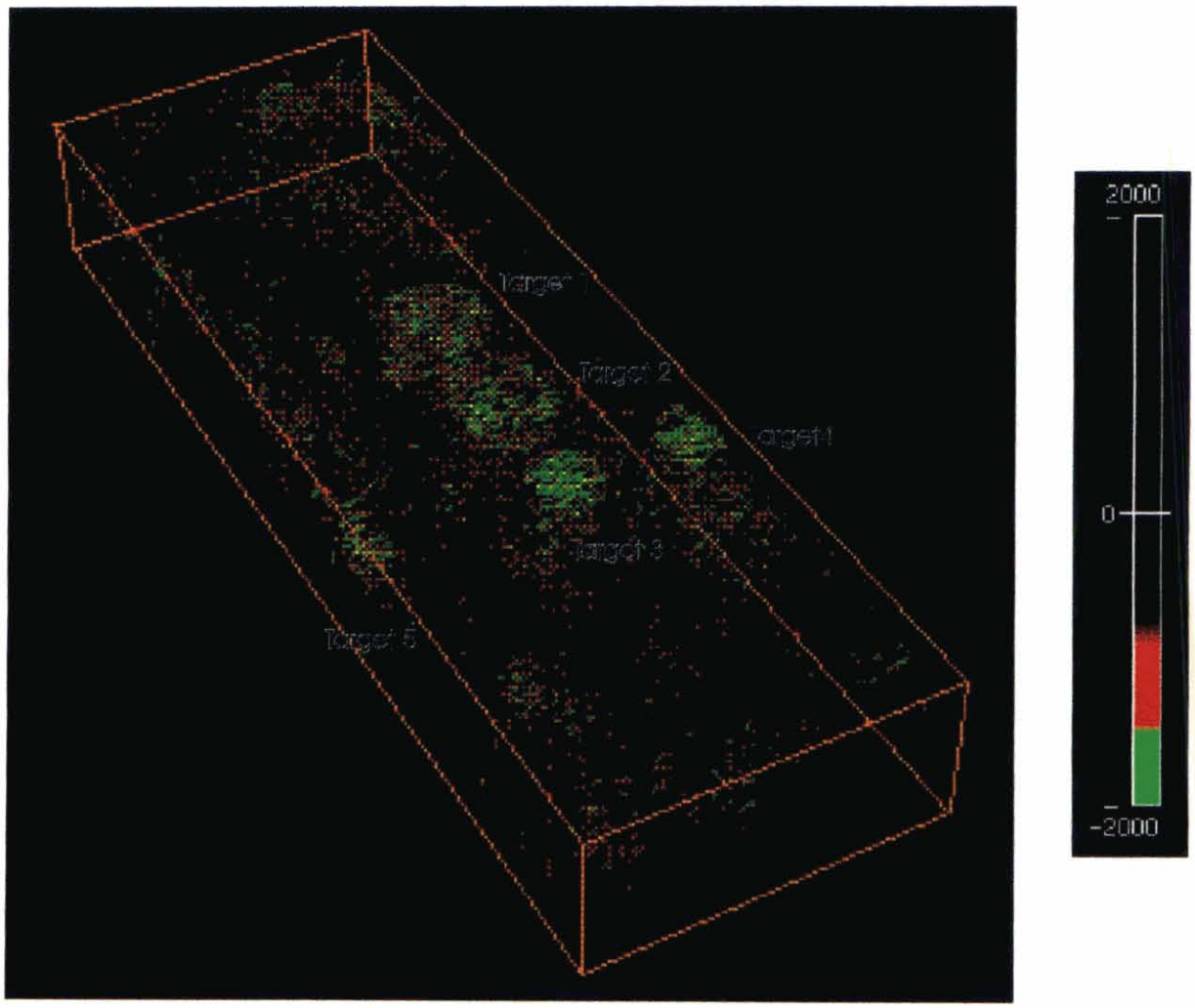

Figure 15

A three-Dimensional GPR image of the Baker Wood Creosoting site.

Electromagnetic Results

Two-Dimensional Profiles and Contour Interpretation

The two-dimensional profiles of the EM data collected at the Baker Wood Creosoting site, with the frequencies 2 kHz in phase, 4 kHz in phase, and 9kHz in phase, has several anomalies shown. In figure 8a, two creosote tank pads are seen as a decrease in the secondary field between station numbers 21 and 30 and again between station numbers 45 and55. There is also a decrease in the secondary field between station numbers 7 and 15. This anomaly has depth and may be another creosote tank pad. The anomaly was not drilled and confirmed. Figure 8b has a decrease in the secondary field between stations 17 and 37. This anomaly is a creosote tank pad. Also there is an anomaly between stations 5 and 9. The anomaly does have depth to it but because the anomaly was not drilled, it is hard to tell what the anomaly is. Figure 9 shows decrease in the secondary field and is a creosote tank pad. Also the figure shows two other anomalies between stations 5 and 9 and between 45 and 53. These anomalies were not drilled but could be creosote filled trenches.

The in-phase and out-of-phase contour maps of the EM data are shown in Figures 10 and 11 respectively. In the in-phase contour maps (figure 10), only two of the creosoting tank pads can be seen readily. This is probably due the amount of rebar in the creosote tank pads with the highest amount in the two readily seen creosote tank pads. The conductivity of the ground is shown in the out-of-phase contour maps in Figure 11. The out-of-phase contour maps are not readily interpretable. In the NW area there is conductive soil and represents where there was standing water.

Interpretation of EM Data In Conjunction With GPR

The EM and GPR images of the subsurface at the Baker Wood Creosoting site differ in resolution. The EM data is not readily interpretable, with many of the site anomalies missing from the EM images. Many of the anomalies from the EM data were only detected by employing the GPR data. Also the EM data does not readily show the spatial extent of the PAH compounds. Where as the GPR images are readily interpretable, showing the location and sometimes the identification of the anomalies.

Conclusions

The mapping of the spatial extent of PAH compounds by EM and GPR was successful at the Baker Wood Creosoting site and imaged several anomalies. They imaged such objects as: 1) at least five creosote tank pads, 2) creosote sitting underneath the tank pads, 3) several creosote filled pits, 4) maybe several pipes, and 5) some asphalt at the site.

The orientation of the GPR antennas must be considered for each site surveyed. A dipole GPR antenna radiates linearly polarized waves. The electric field contains a vector that is oriented parallel to the long axis of the transmitting antenna. Due to the reciprocity theorem, the receiving antenna is most sensitive to the electric field vector oriented parallel to its long axis and the antenna must be oriented such that it receives the highest amount of reflected energy.

GPR can be readily interpretable by employing three-dimensional images. The process of producing a three-dimensional image is an essential part of the overall interpretation. The selection of amplitude-color assignment, the amount of data to be displayed, and the optimum viewing angle of the display are determined simultaneously with the interpretation to produce the best three-dimensional data block (Daniels, 1997).

The EM and GPR images of the surveyed site differ in resolution. The EM images are not readily interpretable, with a majority of the anomalies missing from the two-dimensional profiles and contour maps. Also from the EM images, one can not determine the spatial extent or detect PAH compounds with in the site. Where as the GPR images are readily interpretable, showing the locations of anomalies.

References

Bob, 1995, AHPCRC BOB Program Manual: University of Minnesota Army High Performance Computing Re4search Center, Army Research Office Contact number DAAL 03-89-C-0038.

Bookshar, J., 1998, GPR: Antenna Effects and Patterns: BS Thesis, OSU., Col., Oh.

Coruh, C., Robinson, E.S., 1988, Basic Exploration Geophysics: John Wiley and Sons, N.Y., N.Y., p. 490-492.

Daniels, J.J., 1989, Fundamentals of Ground Penetrating Radar, Proceedings of SAGEEP, Golden, Colorado.

Daniels, J.J., Roberts, R.L., 1996, Analysis of GPR Phenomena, JEEG, vol. 1, issue 2, p. 139-157.

Daniels, J.J., Grumman, D.L., Vendl, M.A., 1997, Coincident Antenna Three-Dimensional GPR, JEEG, vol. 2, issue 1, p. 1-9.

Guy, E.D., 1999, Demonstration of Using Crossed Dipole GPR Antenna for Site Characterization, Submitted to "Geophysical Research Letters" AGG, May 15, 99.

Grumman, 1995, Radical

Keckler, D., 1995, Surfer for Windows: Golden Software Inc., Golden, Colorado, p. 3.3-3.6.

Klein, J., Lajoie, J., 1980, Practical Geophysics: Northwest Mining Ass., Spokane, WA, p. 240-244.

Morrison, T.M., 1918, Soil Survey of Marion County, Oh.: Government Printing Office, Washington, p. 5-9.

Ohio Environmental Protection Agency (Ohio EPA), Division of Emergency and Remedial Response, 1998, Integrated Assessment Report and Baker Wood Creasoting, Marion, Oh., ID# OH 001 326 610.

Roberts, R.L., 1994, Analysis and Theoretical Modeling of GPR Polarization Data: Ph.D. Dissertation, O.S.U., Col., Oh.